Vasopressin-induced serine 269 phosphorylation reduces Sipa1l1 (signal-induced proliferation-associated 1 like 1)-mediated aquaporin-2 endocytosis

Received for publication, February 2, 2017, and in revised form, March 14, 2017 Published, Papers in Press, March 23, 2017, DOI 10.1074/jbc.M117.779611

Po-Jen Wang[‡], Shu-Ting Lin[‡], Shao-Hsuan Liu[‡], Kuang-Ting Kuo[‡], Chun-Hua Hsu[§], Mark A. Knepper[¶], and Ming-Jiun Yu[‡1]

From the [‡]Institute of Biochemistry and Molecular Biology, National Taiwan University College of Medicine, Taipei 10051, Taiwan, the [§]Department of Agricultural Chemistry, National Taiwan University, Taipei 10617, Taiwan, and the [¶]Systems Biology Center, NHLBI, National Institutes of Health, Bethesda, Maryland 20892-1603

Edited by Gerald W. Hart

The abundance of integral membrane proteins in the plasma membrane is determined by a dynamic balance between exocytosis and endocytosis, which can often be regulated by physiological stimuli. Here, we describe a mechanism that accounts for the ability of the peptide hormone vasopressin to regulate water excretion via a phosphorylation-dependent modulation of the PDZ domain-ligand interaction involving the water channel protein aquaporin-2. We discovered that the PDZ domain-containing protein Sipa1l1 (signal-induced proliferation-associated 1 like 1) binds to the cytoplasmic PDZ-ligand motif of aquaporin-2 and accelerates its endocytosis in the absence of vasopressin. Vasopressin-induced aquaporin-2 phosphorylation within the type I PDZ-ligand motif disrupted the interaction, in association with reduced aquaporin-2 endocytosis and prolonged plasma membrane aquaporin-2 retention. This phosphorylation-dependent alteration in the PDZ domain-ligand interaction was explained by 3D structural models, which showed a hormone-regulated mechanism that controls osmotic water transport and systemic water balance in mammals.

Integral membrane proteins in the plasma membrane including receptors and transporters are synthesized in the endoplasmic reticulum and are delivered to the plasma membrane to fulfill their functions (1). Their abundance in the plasma membrane is ultimately determined by a balance between exocytosis of the intracellular vesicles that contain them and endocytosis of the plasma membranes where they reside. The balance is subject to regulatory influences that govern proper functions of the integral membrane proteins in time and location. Dysregulation in these regulatory processes are associated with many clinical manifestations including cardiac, metabolic, and neurological disorders (2–4).

Here we report a hormone-regulated mechanism that controls plasma membrane protein abundance via a conserved protein-interacting module known as PDZ domain, where PDZ is an acronym for three proteins, PSD-95 (postsynaptic density protein 95), Dlg (disks large homolog 1), and ZO-1 (zona occludens protein 1) (5). PDZ domains bind to protein COOH-terminal ligand motifs, which are classified into three classes: class I motif Ser/Thr-*X*-Φ, class II motif Φ-*X*-Φ and class III motif Asp/Glu-*X*-Φ (where *X* is any amino acid residue and Φ is any hydrophobic residue)(6). PDZ domains are found in many proteins in yeast, worm, fly, mouse, and human (5). In human, there are 234 PDZ domains present in 126 proteins. Thus, many proteins have more than one PDZ domain and are capable of simultaneous interactions with several proteins that contain PDZ-ligand motifs. Proteins that contain PDZ domains are involved in a variety of biological processes including scaffolding, signaling, and protein trafficking (5).

Aquaporin-2 (AQP2)[2] is a water channel protein in the kidney collecting duct epithelial cells (7). Its activity in the apical plasma membrane is regulated by the antidiuretic peptide hormone vasopressin, thereby controlling the cells' ability to reabsorb water via osmosis. The regulatory action of vasopressin is associated with vasopressin-induced AQP2 phosphorylation on two serine residues at the COOH terminus (8). Serine 256 (Ser-256) phosphorylation is required for apical AQP2 exocytosis (9–11). Ser-269 phosphorylation appears to inhibit AQP2 endocytosis but the mechanism is unknown. In response to vasopressin, Ser-269 undergoes a 9-fold increase in its phosphorylation level, accounting for 26% of all AQP2 molecules in collecting duct cells (12). Ser-269-phosphorylated AQP2 is exclusively found in the apical plasma membrane (13), consistent with an inhibitory role of Ser-269 phosphorylation in AQP2 endocytosis (13, 14). In fact, Ser-269 phosphorylation was found to inhibit AQP2 endocytosis by overriding lysine 270 (Lys-270) polyubiquitylation-mediated endocytosis (15, 16). Further studies alluded to Ser-269 phosphorylation-dependent alteration in protein-protein interactions that result in apical AQP2 retention (17); however, the interacting proteins involved were not identified.

This work was supported by Ministry of Science and Technology, Taiwan Grant MOST-104-2320-B-002-064-MY3 (to M. J. Y.) and National Institutes of Health, NHLBI Project Grants ZIA-HL001285 and ZIA-HL006129 (to M. A. K.). The authors declare that they have no conflicts of interest with the contents of this article. The content is solely the responsibility of the authors and does not necessarily represent the official views of the National Institutes of Health.

[1] To whom correspondence should be addressed: Rm. 816, No. 1 Sec. 1 Jen-Ai Rd., Taipei 10051, Taiwan. Tel.: 886-2-2312-3456 (ext. 88216); Fax: 886-2-3393-1691; E-mail: mjyu@ntu.edu.tw.

[2] The abbreviations used are: AQP2, Aquaporin-2; Sipa1l1, signal-induced proliferation-associated 1 like 1; mpkCCD, mouse kidney collecting duct cell; dDAVP, 1-deamino-8-D-arginine vasopressin.

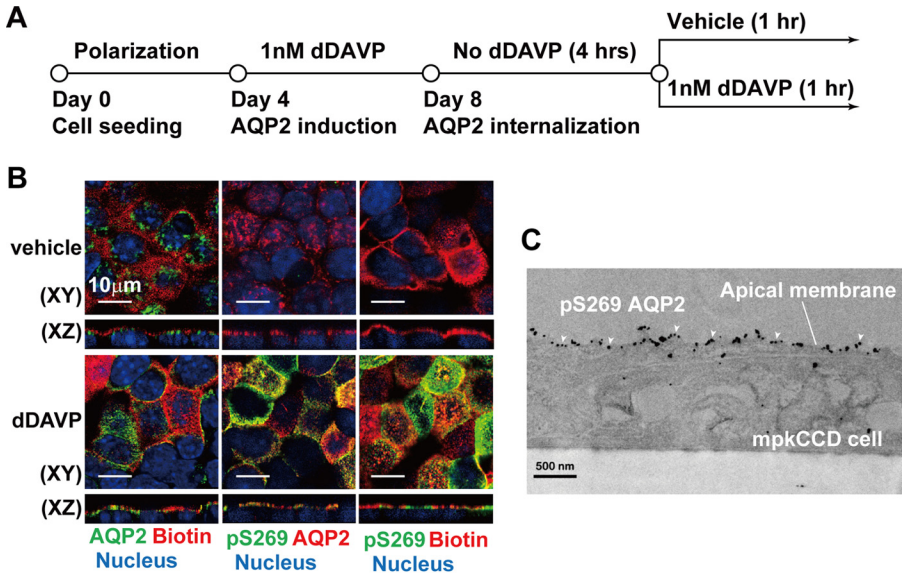

Figure 1. Ser-269 phosphorylation enhanced apical AQP2 retention in the mpkCCD cells. *A,* the experimental protocol. *B* and *C,* confocal immunofluorescence and immuno-EM micrographs of AQP2 in mpkCCD cells in response to the vasopressin V2 receptor-specific analog dDAVP. The apical plasma membrane was labeled with biotin. The cell nuclei were stained with DAPI. *pS269* indicates Ser-269 phosphorylated AQP2 (*arrowheads in C*).

Ser-269 of the AQP2 COOH terminus (SKA) is contained within the class I PDZ-ligand motif (6). Vasopressin-induced AQP2 phosphorylation at Ser-269 adds a negative charge to the class I motif and converts it to a class III-like motif. We hypothesized that this hormone-induced charge change in the AQP2 PDZ motif may alter the interaction of AQP2 with a corresponding PDZ domain-containing protein that is required for AQP2 endocytosis. Using protein mass spectrometry, we identified an apically expressed PDZ domain-containing protein Sipa1l1 (signal-induced proliferation-associated 1 like 1), which interacts with and mediates AQP2 endocytosis in the absence of vasopressin. We further showed that vasopressin-induced phosphorylation of AQP2 at Ser-269 reduced the interaction of AQP2 with and endocytosis by Sipa1l1, prolonging apical AQP2 retention. Our results provide a mechanism that explains vasopressin-mediated regulation of osmotic water transport in the kidney collecting duct cells.

Results

Ser-269 phosphorylation enhanced apical AQP2 retention in the mpkCCD cells

Mouse kidney collecting duct cells (mpkCCD) were chosen to study the molecular mechanism involved in vasopressin-mediated AQP2 trafficking because the cells contain all necessary components for vasopressin-induced endogenous AQP2 expression, phosphorylation, and trafficking (18–20). The cells were seeded on Transwell membrane supports and grown to polarization that segregates the plasma membrane into apical and basolateral membranes (Fig. 1*A*), representing the urine side and the serum side of the kidney collecting ducts. The cells were then treated with the vasopressin V2 receptor-specific agonist dDAVP added to the basolateral side to induce endogenous AQP2 protein expression. Before using the cells for AQP2 trafficking studies, dDAVP was withdrawn so that most AQP2 was in intracellular vesicles. After reapplication of dDAVP, AQP2 was in the apical plasma membrane, co-localizing with biotin that was used to label and delineate the apical plasma membrane (Fig. 1*B*, *bottom left panel*). Without dDAVP reapplication, most AQP2 remained in an intracellular location (Fig. 1*B*, *top left panel*). Without dDAVP reapplication, AQP2 was not phosphorylated at Ser-269 (Fig. 1*B*, *top middle panel*, pS269). Reapplication of dDAVP drastically increased Ser-269 phosphorylation (Fig. 1*B*, *bottom middle panel*). Most Ser-269 phosphorylated AQP2 was in the apical plasma membrane by immunofluorescence (Fig. 1*B*, *bottom right panel*) and immuno-EM staining (Fig. 1*C*).

We next tested whether Ser-269 phosphorylation enhances AQP2 apical retention by examining cellular localization of ectopically expressed phosphorylation-mimicking (serine to aspartate, S269D) and phosphorylation-ablated (serine to alanine, S269A) mutant AQP2 in the mpkCCD cells (Fig. 2*A*) as previously seen in Madin-Darby canine kidney cells (13, 17, 21). As seen in Fig. 2*B*, the S269A mutant AQP2 trafficked to the apical plasma membrane (*middle panels*, pixel overlap best seen in the XZ reconstruction) as the wild-type AQP2 did in response to dDAVP (*left panels*), suggesting that Ser-269 phosphorylation is not required for apical AQP2 exocytosis. In contrast, the S269D mutant AQP2 was already localized in the apical plasma membrane in the absence of dDAVP (Fig. 2*B*, *top right panel*), consistent with a role of Ser-269 phosphorylation in apical AQP2 retention. Fig. 2*C* shows our image analysis method, and Fig. 2*D* summarizes the results.

Apical membrane proteomics identified candidate AQP2-interacting PDZ domain-containing proteins

There are 126 and 78 annotated PDZ domain-containing proteins in the human and mouse genome, respectively (5). To narrow down potential candidates that could interact with the AQP2 COOH-terminal motif, we analyzed the published transcriptome and proteome databases of rat kidney collecting ducts (22, 23) and cultured mpkCCD cells (18, 20) for proteins

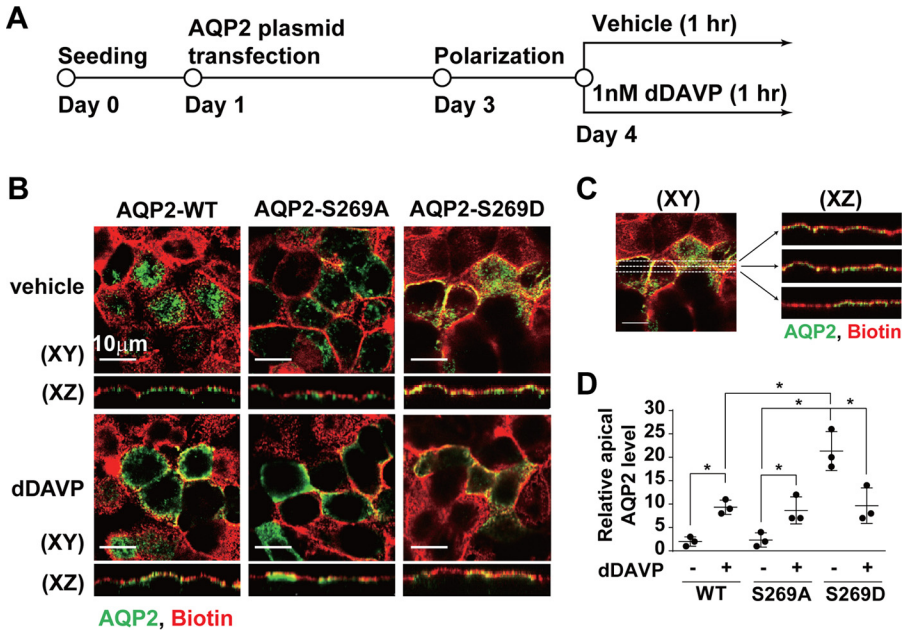

Figure 2. Phosphorylation-mimicking mutation at Ser-269 enhanced apical AQP2 retention in the mpkCCD cells. *A,* the experimental protocol. *B,* confocal immunofluorescence micrographs of the wild type (WT), S269A and S269D mutant AQP2 in mpkCCD cells stimulated with vehicle or dDAVP for 1 h. The apical plasma membrane was labeled with biotin. *C,* the image analysis protocol. Three lines were drawn across each X-Y plane image to produce three X-Z plane images. Relative apical AQP2 level was calculated as the AQP2 pixels that overlapped with the biotin pixels divided by the total AQP2 pixels. *D,* a scatter plot summarizing the imaging results. Values are mean ± S.D. *Asterisk* indicates significance $p < 0.05$, *t* test.

with annotated PDZ domains in the NCBI conserved domain database. Fifty-two PDZ domain-containing proteins were found in the two cell types. Because both cell types exhibit similar vasopressin-mediated AQP2 regulation, the PDZ domain-containing proteins common to both cell types made them good AQP2-interacting candidates. We next reasoned that apically expressed PDZ domain-containing proteins are better candidates to mediate apical AQP2 trafficking and analyzed the apical membrane proteomes of rat kidney collecting ducts (24) and mpkCCD cells in this study (the mpkCCD Apical Membrane Proteome Database). Altogether, 5 PDZ domain-containing proteins were identified in the apical membrane proteome of collecting duct cells. Of these, four are common to both cell types, *viz.* Golgi-associated PDZ and coiled-coil motif-containing protein (Gopc), MAGUK p55 subfamily member 5 (Mpp5), PDZ domain-containing RING finger 3 (Pdzrn3), and Sipa1l1.

To predict potential binding motifs, we used the BLAST program to align the PDZ domain sequences to those in a database of PDZ domains whose binding motifs have been characterized (25). Fig. 3*A* summarizes the PDZ domain structures and the predicted binding motif logos. As seen, the PDZ domain of Gopc is most similar to the PDZ domain of human α1 syntrophin, which binds a motif logo similar to the AQP2 motif logo (Fig. 3*B*). The Sipa1l1 PDZ domain is most similar to the human SHANK3 PDZ domain that binds a motif logo similar to the AQP2 motif logo. The PDZ domain of Mpp5, the two PDZ domains of Pdzrn3, and the PDZ domain of Sipa1, a PDZ domain-containing protein previously shown to mediate AQP2 exocytosis (26), were predicted not to bind the AQP2 motif in our analysis.

Sipa1l1 interacted with and mediated AQP2 endocytosis

Immunoblotting results showed that Gopc, Mpp5, and Sipa1l1 were expressed in the mpkCCD cells (Fig. 4, *A*, *C*, and *E*). Pdzrn3 was not detected due to the lack of an antibody of sufficient quality. Gopc and Sipa1l1 proteins were readily detectable in the total cell lysate, whereas Mpp5 protein was detected in the 17,000 × *g* membrane fraction. Exposure to 1 nM dDAVP for 1 h did not affect the protein levels of Gopc, Mpp5, and Sipa1l1 in the cells. On immunofluorescence confocal micrographs, Gopc and Mpp5 showed discrete intracellular localization from that of AQP2 (Fig. 4, *B* and *D*), whereas Sipa1l1 showed partial co-localization with AQP2 (Fig. 4*F*), suggesting potential interaction between Sipa1l1 and AQP2 in the mpkCCD cells. Indeed, co-immunoprecipitation using the AQP2 antibody followed by immunoblotting for Sipa1l1 showed results consistent with an interaction between AQP2 and Sipa1l1. Sipa1l1 was detected in the AQP2 immunoprecipitate of the mpkCCD cells expressing AQP2 and not in the AQP2 immunoprecipitate of the cells not expressing AQP2 (Fig. 5*A*). To examine functions of Sipa1l1 in AQP2 localization, Sipa1l1 was knocked down in the mpkCCD cells with two small hairpin RNA sequences (Fig. 5*B*) followed by immunofluorescence staining for AQP2 localization (Fig. 5*C*). As seen, most AQP2 was intracellular in the control cells before dDAVP stimulation (*top left panel*). Upon dDAVP stimulation, AQP2 trafficked to the apical membrane of the control cells (Fig. 5*C*, *bottom left panel*). In contrast, AQP2 was already in the apical plasma membrane in the Sipa1l1 knockdown cells without dDAVP stimulation (Fig. 5*C*, *top right panel*). Without dDAVP stimulation, AQP2 was intracellular in the control cells (Fig. 5*C*, *top left panel*). Fig. 5*D* summarizes the imaging results. To ver-

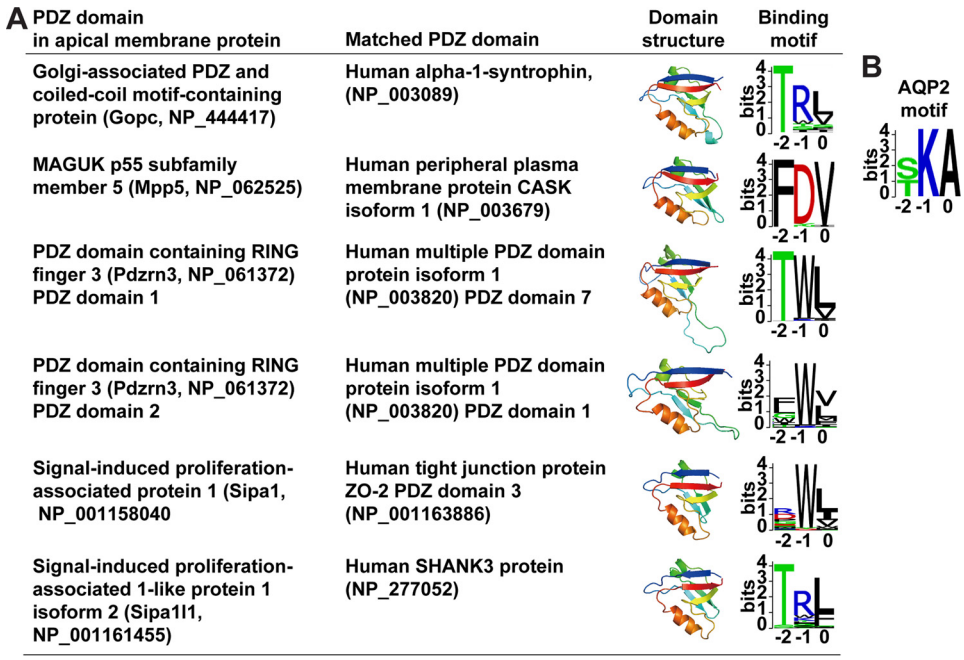

Figure 3. Predicted PDZ domain structures and their binding motif logos. *A,* the PDZ domain structures of Gopc, Mpp5, Pdzrn3, Sipa1, and Sipa1l1 were predicted using SWISS-MODEL online software. The corresponding binding motifs were predicted by BLAST alignment of the PDZ domains with those in a PDZ domain library whose binding motifs have been characterized (25). Pdzrn3 has two PDZ domains. *B,* AQP2 motif logo.

ify the imaging results, apical surface biotinylation coupled with streptavidin affinity purification and immunoblotting was used to compare the amounts of apical AQP2 in the control and the Sipa1l1 knockdown cells under the vehicle conditions (Fig. 5*E*). As seen, less apical AQP2 was detected in the control than in the Sipa1l1 knockdown cells under the vehicle conditions, consistent with a role of Sipa1l1 in AQP2 endocytosis in the absence of vasopressin.

Ser-269 phosphorylation reduced AQP2-Sipa1l1 interaction and AQP2 endocytosis

If Sipa1l1 mediates AQP2 endocytosis in the absence of vasopressin, one hypothesis for Ser-269 phosphorylation-mediated apical AQP2 retention is that there is a reduced interaction of AQP2 with Sipa1l1 when AQP2 is phosphorylated at Ser-269, thereby reducing endocytosis. The above hypothesis would predict a reduced binding preference of Sipa1l1 toward Ser-269-phosphorylated *versus* non-phosphorylated AQP2 peptides (Fig. 6*A*). Consistent with this, the Ser-269-phosphorylated AQP2 peptide was less capable of pulling down Sipa1l1 in the mpkCCD cell lysate compared with Ser-269 non-phosphorylated AQP2 peptide (Fig. 6, *B* and *C*). A similar binding preference was observed at the whole AQP2 protein level. AQP2 protein was immunoprecipitated from S269D or S269A AQP2 protein expressing mpkCCD cells before the amounts of Sipa1l1 bound to them were measured with immunoblotting. As seen in Fig. 6, *D* and *E*, the amount of Sipa1l1 bound to S269D AQP2 protein was significantly less than that bound to S269A AQP2 protein, consistent with a reduced Sipa1l1 binding with Ser-269-phosphorylated AQP2 protein. Because Sipa1l1 had a reduced binding preference for S269D AQP2, Sipa1l1 knockdown did not have apparent effects on the apical localization of S269D AQP2 in the absence of dDAVP (Fig. 6*F*, *right panel*). In contrast, Sipa1l1 knockdown resulted in apical localization of S269A AQP2 in the absence of dDAVP (Fig. 6*G*, *right panel*). In the absence of dDAVP, S269A AQP2 was intracellular in the control cells (Fig. 6*G*, *left panel*).

Models show reduced interaction between Ser-269-phosphorylated AQP2 and Sipa1l1

To provide a molecular basis of the PDZ interaction between Sipa1l1 and AQP2, we modeled the structure of the Sipa1l1 PDZ domain based on the crystal structure of the NHERF PDZ domain for two reasons (27). 1) The NHERF PDZ domain binds type I (Ser/Thr-*X*-Φ) ligands Ser-Leu-Leu of the β2 adrenergic receptor and Ser-Phe-Leu of the platelet-derived growth factor receptor, similar to Ser-Lys-Ala of the murine AQP2 ligand motif. 2) Both NHERF and Sipa1l1 have PDZ domains with similar sequences in the loop between the β1 and β2 strands, which forms a binding pocket for the terminal carboxylate of the motif (28). As seen in the model (Fig. 7*A*), the AQP2 motif (PRGSKA) backbone lies in the groove (*left panel*) between the β2 strand and the α2 helix of the PDZ domain (*right panel*), forming hydrogen bonds with the backbone of the β2 strand (29). In the model, the positive charged arginine 267 side chain of AQP2 forms salt bridges with the negatively charged glutamate side chain on the α2 helix (Fig. 7*A*, *right panel*). In addition, the positive Lys-270 side chain of the AQP2 motif points at the negative aspartate and glutamate side chains on the β3 strand of the Sipa1l1 PDZ domain, further strengthening the interaction. Note that Lys-270 points outward away from the Sipa1l1 PDZ domain and allows it to be ubiquitylated (Fig. 7*C*) (15, 16). Thus, Lys-270-ubiquitylated AQP2 could still bind the Sipa1l1 PDZ domain. In addition, Lys-270 and Ser-269 point at different angles. Therefore, Lys-270 ubiquitylation and Ser-269 phosphorylation are not mutually exclusive. The -OH group of

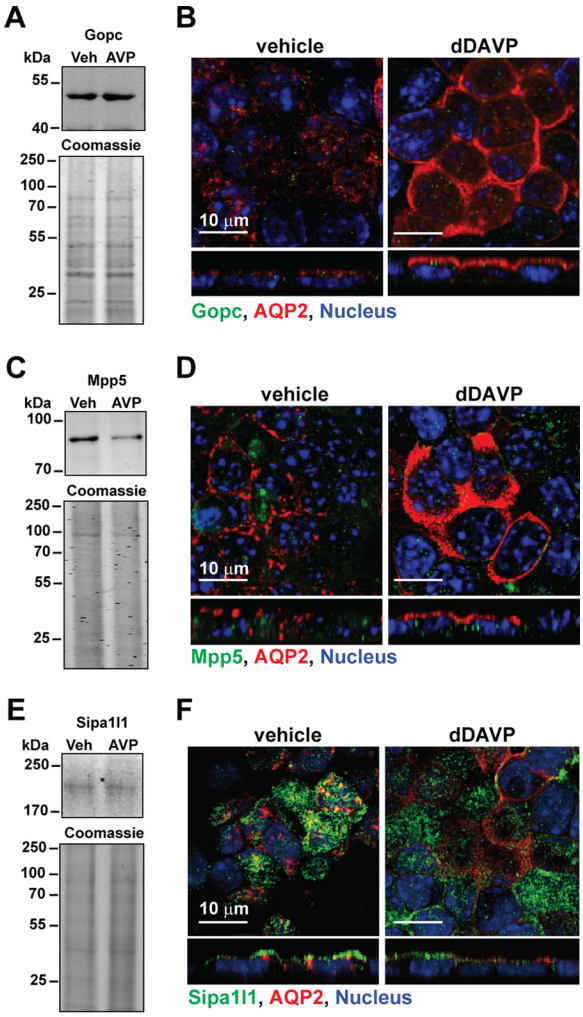

Figure 4. Expression of three PDZ domain-containing proteins in the mpkCCD cells. *A*, *C*, and *E*, immunoblotting, and *B*, *D*, and *F*, confocal immunofluorescence staining for Gopc, Mpp5, and Sipa1l1 in the mpkCCD cells in response to vehicle (*Veh*) or 1 nM dDAVP (*AVP*) for 1 h.

the Ser-269 side chain of the AQP2 motif forms a hydrogen bond with N3 of the imidazole ring of the conserved histidine side chain of the α2 helix (Fig. 7*A*, *right panel*) (28). Phosphorylation of the -OH group creates a steric hindrance against the histidine side chain and adds a negative charge toward the hydrophobic isoleucine side chain on the α2 helix (Fig. 7*B*). Both are expected to destabilize the interaction between the Ser-269-phosphorylated AQP2 motif and the Sipa1l1 PDZ domain. Modeling using the human AQP2 motif PRGTKA yielded similar results.

Discussion

In this study, we describe a mechanism that controls the abundance of a membrane protein in the plasma membrane via the cytoplasmic COOH-terminal motif of the membrane protein. Cytoplasmic motifs of plasma membrane proteins often serve as signals for intracellular trafficking via interactions with adaptor proteins at various locations including the trans-Golgi network, plasma membrane, and recycling endosomes (30, 31). In the present case, we found that the cytoplasmic COOH-terminal motif of AQP2 serves as a signal for endocytosis mediated by the PDZ domain-containing protein Sipa1l1 (Fig. 5*C*). In addition to signaling for endocytosis, the AQP2 COOH-terminal motif also regulates AQP2 abundance in the apical plasma membrane via a phosphorylation-dependent reduction in its interaction with and endocytosis by Sipa1l1 (Fig. 6). This phosphorylation-dependent reduction in the AQP2-Sipa1l1 interaction is stimulated by the peptide hormone vasopressin, which induces phosphorylation of Ser-269 in the AQP2 motif and disrupts a critical hydrogen bond between the AQP2 COOH-terminal motif and the Sipa1l1 PDZ domain (Fig. 7). By disrupting the AQP2 interaction with Sipa1l1, vasopressin reduces AQP2 endocytosis thereby increasing AQP2 retention in the apical plasma membrane and osmotic water reabsorption by the cells. Phosphorylation at the serine or threonine residue of the class I motif has been shown to disrupt PDZ interactions of the inward rectifier K channel Kir 2.3 (32), β2-adrenergic receptor (33), and stargazin (34) with their respective PDZ domain proteins. The consequences of the disruption include dissociation of the channel from the cytoskeleton (32) and impaired surface expression of the receptors (33, 34). Thus, the phosphorylation-mediated switch from the class I to class III-like PDZ motif could serve as a general mechanism to regulate surface expression of membrane proteins and their physiological functions.

Vasopressin-induced AQP2 phosphorylation at Ser-269 was first demonstrated by phosphoproteomics in 2006 (35). Several studies have supported the view that this phosphorylation event plays a key role in AQP2 trafficking in collecting duct cells (12–14, 17). The current model favors reduced AQP2 endocytosis upon Ser-269 phosphorylation that overrides polyubiquitylation-mediated AQP2 endocytosis via an unknown mechanism (13–16). Our data provide a new regulatory mechanism that explains how vasopressin-induced Ser-269 phosphorylation facilitates retention of AQP2 in the apical plasma membrane.

How does Sipa1l1 mediate AQP2 endocytosis? We speculate a potential mechanism based on the molecular structure and prior knowledge on Sipa1l1 (36, 37). Sipa1l1 is also known as SPAR (spine-associated Rap GTPase-activating protein) in rats (37). It contains a PDZ domain, a RapGAP domain, a guanylate kinase-binding domain, and two actin-interacting domains. In rat neurons, SPAR, via its PDZ domain, binds the COOH terminus of the ephrin-A receptor and activates the RapGAP domain. The activated RapGAP promotes hydrolysis of Rap1 (Ras-related protein 1)-bound GTP to GDP thereby inactivating Rap1. This results in actin reorganization and leads to growth cone collapse (36). In the context of AQP2 endocytosis, we propose the following mechanism. Upon vasopressin removal (Fig. 8*A*), Ser-269 is dephosphorylated. This permits Sipa1l1 binding to the COOH-terminal motif of AQP2 at the apical plasma membrane and results in RapGAP activation. The activated RapGAP hydrolyzes Rap1-bound GTP to GDP and inactivates Rap1, leading to reorganization of cortical actin skeleton locally at the apical plasma membrane. The cortical actin skeleton on one hand, via interactions with integral membrane proteins, supports the shape of the plasma membrane and regulates the functions of integral membrane proteins. The cortical actin skeleton, on the other hand, creates barriers for

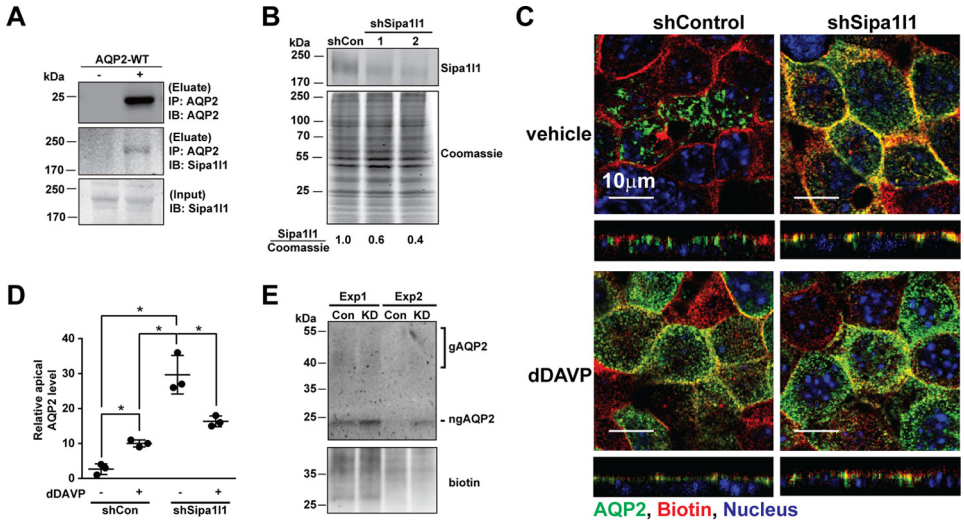

Figure 5. Sipa1l1 participated in AQP2 endocytosis. *A,* immunoprecipitation (*IP*) followed by immunoblotting (*IB*) for testing AQP2-Sipa1l1 interaction. The mpkCCD cells were transfected with or without the wild-type AQP2 expression vector before the cell lysates were subjected to immunoprecipitation with the AQP2 antibody followed by immunoblotting for AQP2 and Sipa1l1. *B,* representative immunoblotting for Sipa1l1 in non-targeted control (*shCon*, TRCN0000072246: CAAATCACAGAATCGTCGTAT) and Sipa1l1 knockdown (shSipa1l1) mpkCCD cells. Two shSipa1l1 sequences (TRCN0000106106, GCCATTATGAACAGACATAAT; and TRCN0000106109, CGCCACTAGCAAATATCTGAT) were used for the knockdown. The Sipa1l1 band intensity was measured with the LiCor Odyssey scanner and normalized with Coomassie staining. Sipa1l1 knowndown efficiency is indicated. Three independent experiments were performed. *C,* confocal immunofluorescence staining for AQP2 in control and Sipa1l1 knockdown mpkCCD cells in response to vehicle or 1 nM dDAVP for 1 h. *D,* a scatter plot of the imaging results. The analysis method was described above in Fig. 2*C*. Values are mean ± S.D. *Asterisk* indicates significance $p < 0.05$, *t* test. *E,* immunoblotting for apical AQP2. The mpkCCD cells, control (*Con*) or Sipa1l1 knockdown (*KD*), under the vehicle control conditions were labeled with apical surface biotinylation before the labeled protein was purified with streptavidin affinity chromatography for immunoblotting and biotin staining. Two experiments (*Exp 1* and *2*) were done. *gAQP2*, glycosylated AQP2; *ngAQP2*, non-glycosylated AQP2.

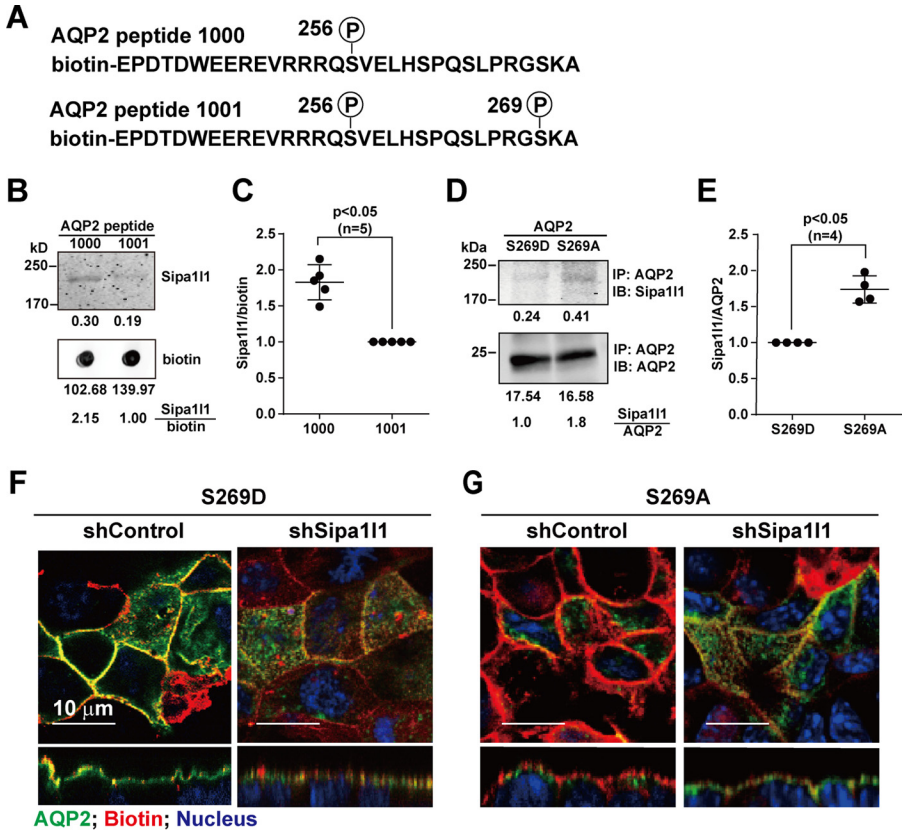

Figure 6. Sipa1l1 preferentially interacted with Ser-269 non-phosphorylated AQP2. *A,* biotin-labeled synthetic AQP2 COOH-terminal peptides. *B* and *C,* representative immunoblot (*IB*) and summary of Sipa1l1 interaction with Ser-256 phosphorylated *versus* Ser-256 and Ser-269 doubly phosphorylated AQP2 peptide. The mpkCCD cell lysate was incubated with the biotin-labeled AQP2 peptides. After binding and washes, the eluate was detected for Sipa1l1 with immunoblotting. *Numbers* are signal intensities (means ± S.D.). *Asterisk* indicates significance, $p < 0.05$, *t* test. *D* and *E,* representative immunoblot and summary of Sipa1l1 interaction with S269A *versus* S269D AQP2 protein. The cell lysates from S269A or S269D AQP2 expressing mpkCCD cells were immunoprecipitated (*IP*) with the AQP2 antibody before immunoblotting for Sipa1l1. *F* and *G,* immunofluorescence staining for S269D and S269A AQP2 in control and Sipa1l1 knockdown mpkCCD cells in the absence of dDAVP.

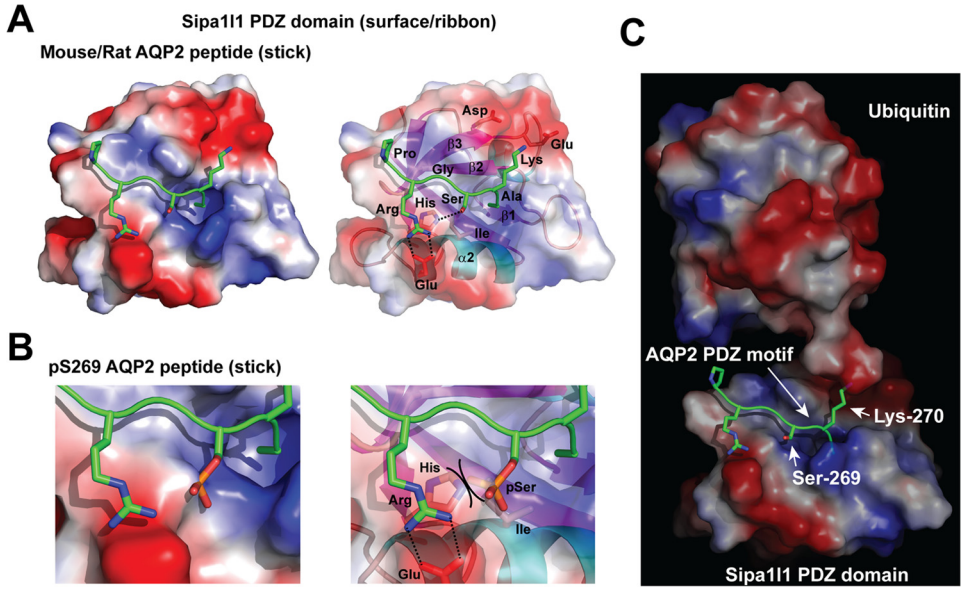

Figure 7. Structural models of the Sipa1l1 PDZ domain. *A,* Sipa1l1 PDZ domain interacting with non-phosphorylated AQP2 peptide. The Sipa1l1 PDZ domain is consisted of β1, β2, β3, α1, β4, β5, α2, and β6 secondary structures shown as a space-filled surface (*left panel*) and a ribbon schematic model (*right panel*). Positive, electroneutral, and negative surfaces are colored *blue*, *white*, and *red*, respectively. The murine AQP2 motif -PRGSKA is shown as *sticks*. Nitrogen, oxygen, and phosphorus are colored *blue*, *red*, and *orange*, respectively. *B,* a blowup model of the Sipa1l1 PDZ domain colliding the Ser-269-phosphorylated AQP2 peptide. Steric hindrance between the phosphorylated Ser (*pSer*) and the His side chain is indicated (*right panel*). *C,* a model of ubiquitylation at Lys-270 of the AQP2 COOH-terminal peptide bound by the Sipa1l1 PDZ domain.

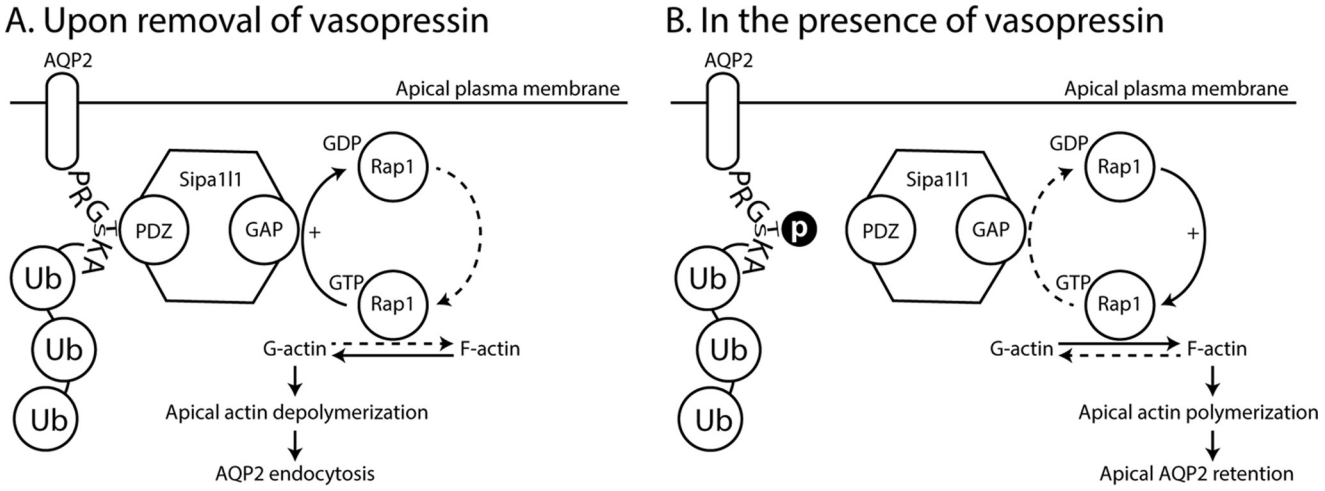

Figure 8. A model of Sipa1l1-meidated AQP2 endocytosis in the kidney collecting duct cells. *A,* upon removal of vasopressin, Sipa1l1 binds Ser-269 (or Thr-269) dephosphorylated AQP2 in the apical plasma membrane and reorganizes cortical actin locally around the apical AQP2, allowing Lys-270 polyubiquitylation-mediated endocytosis to occur. *B,* in the presence of vasopressin, Ser-269 (or Thr-269) phosphorylation reduces Sipa1l1 interaction with AQP2. This shifts cortical actin toward polymerization and slows AQP2 endocytosis. *F-actin*, filamentous actin; *G-actin*, globular actin; *GAP*, RapGTPase activating domain; PDZ, PDZ domain; *Rap1*, Ras-related protein 1; *Ub*, ubiquitin.

endocytosis and exocytosis at the plasma membrane. Reorganizing the cortical actin skeleton locally surrounding apical AQP2 after Rap1 inactivation will be expected to facilitate AQP2 endocytosis upon vasopressin removal.

Numerous studies have demonstrated indispensable roles of actin dynamics in AQP2 trafficking (19, 38–42). Non-muscle myosin II is a versatile protein family of actin-based molecular motors involved in many cellular processes including endocytosis (43). Although the mechanisms involved have not been resolved, non-muscle myosin II is thought to mediate actin contractile activity required for phagocytic cup assembly, squeezing, and closure of receptor-mediated phagocytosis (44, 45). Thus, it is plausible that Rap1 inactivation-mediated cortical actin skeleton reorganization plus non-muscle myosin II-mediated endocytosis could work in concert for AQP2 endocytosis upon vasopressin removal. Non-muscle myosin II, myosin regulatory light chain, and myosin light chain kinase have been implicated in actin reorganization and AQP2 trafficking in collecting duct cells (46, 47). Rap1a and Rap1b are both expressed at very high levels in the rat inner medullary collecting duct (23) and in mpkCCD cells (20, 48). Vasopressin stimulation results in a reduction of Rap1b abundance in the 17,000 × *g* membrane fraction with a reciprocal increase in the 200,000 × *g* cytosolic fraction (49). Hypothetically upon removal of vasopressin, Rap1b may be recruited from the 200,000 × *g* cytosolic fraction to the 17,000 × *g* membrane fraction to regulate cortical actin

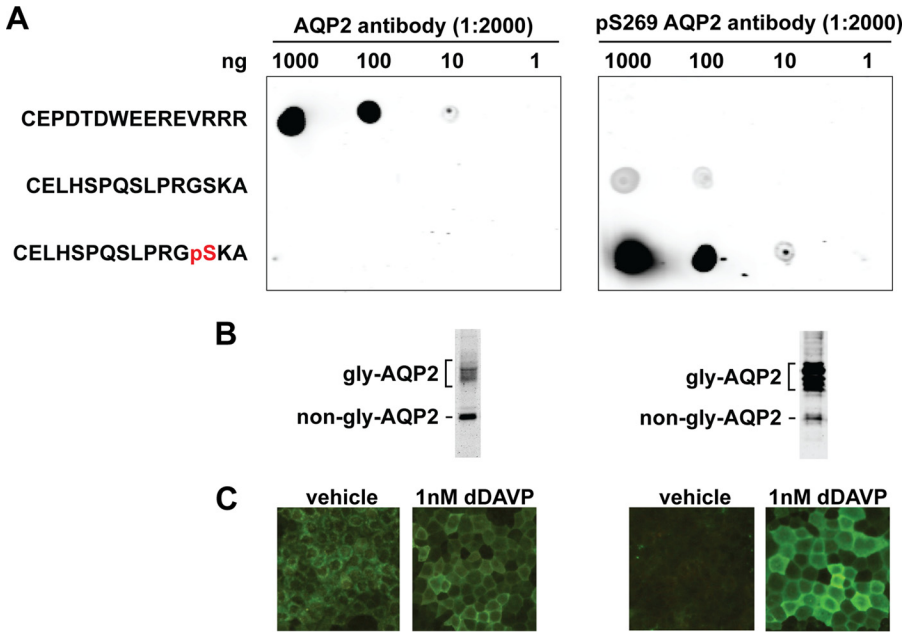

Figure 9. AQP2 antibody characterization. *A,* dot blot tests for the specificity of the antibodies raised against the immunizing AQP2 peptide (CEPDTDWEEREVRRR) and the Ser-269-phosphorylated (*pS269*) AQP2 peptide (CELHSPQSLPRGpSKA). Serial diluted peptides were dotted on nitrocellulose membranes and incubated with the antibodies before detection. *B,* immunoblotting tests for the antibodies. Protein samples were from the mpkCCD cells exposed to dDAVP (1 nM) for 4 days. *Gly-AQP2*, glycosylated; *non-gly-AQP2*, non-glycosylated AQP2. *C,* immunofluorescence staining tests for the antibodies. The mpkCCD cells went through the experimental protocol shown in Fig. 1*A*.

dynamics and AQP2 endocytosis. In addition, AQP2 Lys-270 polyubiquitylation-mediated endocytotic processes (16) could be facilitated when the cortical actin depolymerizes upon vasopressin removal.

In the presence of vasopressin (Fig. 8*B*), Ser-269 is phosphorylated. Sipa1l1 does not bind the AQP2 COOH terminus. The cortical actin dynamics shifts toward actin polymerization and prevents AQP2 endocytosis, despite a high level of Lys-270 polyubiquitylation (15).

Another PDZ domain-containing protein known to mediate apical AQP2 surface expression is SPA-1 (26). SPA-1 (RefSeq accession, NP_001004089) and Sipa1l1 (RefSeq accession, NP_766167) are homologous proteins of different genes. SPA-1 deficiency results in a reduction in apical AQP2 abundance (26), presumably because SPA-1 is required for apical AQP2 exocytosis. SPA-1 was found to bind AQP2 and to form a force-generating protein complex that includes actin, tropomyosin, myosin heavy chain, myosin light chain, and proteins that regulate actin filaments (50). It was believed that SPA-1 binding to intracellular AQP2 activates the RapGAP domain and promotes local actin depolymerization, which facilitates apical AQP2 exocytosis (51). In contrast to the role of SPA-1 to regulate AQP2 exocytosis, our study showed that Sipa1l1 regulates AQP2 endocytosis.

Experimental procedures

Cell culture

The mpkCCD cells re-cloned for the highest AQP2 expression levels were maintained as described previously (20) and used in all experiments. The HEK293T cells for lentivirus production were maintained in DMEM containing 10% fetal bovine serum.

Immunoblotting, confocal immunofluorescence, and immunoelectron microscopy

Detailed procedures for immunoblotting were described previously (19). Commercially available primary antibodies were Gopc (8576S, Cell Signaling), Mpp5 (ab77697, Abcam), and Sipa1l1 (SC31615 or SC20846, Santa Cruz Biotechnology). The chicken antibody was characterized previously (52). Two rabbit polyclonal antibodies against AQP2 and Ser-269-phosphorylated AQP2 peptides were custom-made by GeneTex, Taiwan, and characterized (Fig. 9). The secondary antibodies from Invitrogen were Alexa 488- or 568-conjugated. IRDye 700- or 800-conjugated antibodies were from LiCor. Immunofluorescence staining and immunogold staining were done as previously described (19). Confocal images were acquired with the Leica TCS SP5 microscope and processed with the Leica LAS-AF software or ImageJ software (53).

Apical surface biotinylation

To delineate the apical plasma membrane, glycan-reactive biocytin hydrazide was used to label glycosylated proteins in the apical plasma membrane as described previously (19). Biotin labels were visualized with Alexa 568-conjugated streptavidin. In some cases, the biocytin hydrazide-labeled apical membrane proteins were subjected to streptavidin purification followed by staining for biotin and AQP2.

Apical membrane proteomics

The apical membrane proteins were labeled with sulfo-NHS-LC-biotin and purified with streptavidin affinity chromatography before being subjected to LC-MS/MS-based analysis as detailed previously (24).

Small hairpin RNA-mediated gene knockdown

Plasmids containing small hairpin RNA (shRNA) sequences were packaged into lentivirus particles for stable shRNA-mediated gene knockdown in the mpkCCD cells prior to experiments.

Interaction assays

The mpkCCD cells transfected with or without the wild-type AQP2 expression vector were grown to polarization on membrane supports before the cells were lysed for immunoprecipitation using the AQP2 antibody. Proteins co-precipitated were subjected to immunoblotting for Sipa1l1.

NH_2 terminally biotin-labeled AQP2 peptides (1000, Ser-256 phosphorylated; 1001, Ser-256 and Ser-269 doubly phosphorylated) were used to interact with the polarized mpkCCD cell lysates before immunoblotting for Sipa1l1. In separate experiments, S269A or S269D mutant AQP2 proteins were immunoprecipitated from the mpkCCD cells expressing either mutant before immunoblotting for Sipa1l1.

Molecular modeling

The three-dimensional structure of the mouse Sipa1l1 PDZ domain was generated with the software MODELLER (54) using the X-ray structure of the NHERF PDZ domain (PDB code 1GQ5)(27) as a template. AQP2 peptide (PRGSKA) docking onto the Sipa1l1 PDZ domain was performed using the Rosetta FlexPepDock server (55). The structure of the PDZ-peptide complex was further subjected to a 50-ns molecular dynamics simulation for accurate refinement with the use of the GROMACS 4.5.3 and OPLS-AA (optimized potentials for liquid simulations-all atom) force field (56, 57). The stereochemical quality of the predicted model was validated by the PROCHECK program (58).

Author contributions—P. J. W. did most of the experiments (Figs. 1, 2, 4, 5 and 6) and wrote the first draft of the paper. S. T. L. did the surface biotinylation experiment (Fig. 5E). S. H. L. did the PDZ ligand motif prediction (Fig. 3). K. T. K. characterized the AQP2 antibodies (Fig. 9). C. H. H. performed the molecular modeling (Fig. 7). M. J. Y. did the proteomics and the immunogold staining in the laboratory of M. A. K. M. J. Y. conceived and coordinated the study. M. J. Y. and M. A. K. edited the paper. All authors reviewed the results and approved the final version of the paper.

Acknowledgments—We thank Te-Sheng Lin, Nei-Li Chan, and Shiou-Ru Tzeng in the Institute of Biochemistry and Molecular Biology, National Taiwan University College of Medicine, for technical assistance and fruitful discussion. We thank Hua-Man Hsu in the First Core Lab, National Taiwan University College of Medicine, for excellent support in confocal imaging. We thank Marjan Gucek and Guanghui Wang in the NHLBI Proteomics Core Facility for their assistance on protein mass spectrometry.

References

1. Cao, X., Surma, M. A., and Simons, K. (2012) Polarized sorting and trafficking in epithelial cells. *Cell Res.* **22,** 793–805
2. Knepper, M. A., Kwon, T. H., and Nielsen, S. (2015) Molecular physiology of water balance. *N. Engl. J. Med.* **372,** 1349–1358
3. Curran, J., and Mohler, P. J. (2015) Alternative paradigms for ion channelopathies: disorders of ion channel membrane trafficking and posttranslational modification. *Annu. Rev. Physiol.* **77,** 505–524
4. De Matteis, M. A., and Luini, A. (2011) Mendelian disorders of membrane trafficking. *N. Engl. J. Med.* **365,** 927–938
5. Bhattacharyya, R. P., Reményi, A., Yeh, B. J., and Lim, W. A. (2006) Domains, motifs, and scaffolds: the role of modular interactions in the evolution and wiring of cell signaling circuits. *Annu. Rev. Biochem.* **75,** 655–680
6. Stiffler, M. A., Chen, J. R., Grantcharova, V. P., Lei, Y., Fuchs, D., Allen, J. E., Zaslavskaia, L. A., and MacBeath, G. (2007) PDZ domain binding selectivity is optimized across the mouse proteome. *Science* **317,** 364–369
7. Nielsen, S., Frøkiaer, J., Marples, D., Kwon, T. H., Agre, P., and Knepper, M. A. (2002) Aquaporins in the kidney: from molecules to medicine. *Physiol. Rev.* **82,** 205–244
8. Moeller, H. B., Rittig, S., and Fenton, R. A. (2013) Nephrogenic diabetes insipidus: essential insights into the molecular background and potential therapies for treatment. *Endocr. Rev.* **34,** 278–301
9. Fushimi, K., Sasaki, S., and Marumo, F. (1997) Phosphorylation of serine 256 is required for cAMP-dependent regulatory exocytosis of the aquaporin-2 water channel. *J. Biol. Chem.* **272,** 14800–14804
10. Katsura, T., Gustafson, C. E., Ausiello, D. A., and Brown, D. (1997) Protein kinase A phosphorylation is involved in regulated exocytosis of aquaporin-2 in transfected LLC-PK1 cells. *Am. J. Physiol.* **272,** F817–822
11. van Balkom, B. W., Savelkoul, P. J., Markovich, D., Hofman, E., Nielsen, S., van der Sluijs, P., and Deen, P. M. (2002) The role of putative phosphorylation sites in the targeting and shuttling of the aquaporin-2 water channel. *J. Biol. Chem.* **277,** 41473–41479
12. Xie, L., Hoffert, J. D., Chou, C. L., Yu, M. J., Pisitkun, T., Knepper, M. A., and Fenton, R. A. (2010) Quantitative analysis of aquaporin-2 phosphorylation. *Am. J. Physiol. Renal Physiol.* **298,** F1018–1023
13. Hoffert, J. D., Fenton, R. A., Moeller, H. B., Simons, B., Tchapyjnikov, D., McDill, B. W., Yu, M. J., Pisitkun, T., Chen, F., and Knepper, M. A. (2008) Vasopressin-stimulated increase in phosphorylation at Ser-269 potentiates plasma membrane retention of aquaporin-2. *J. Biol. Chem.* **283,** 24617–24627
14. Moeller, H. B., Knepper, M. A., and Fenton, R. A. (2009) Serine 269 phosphorylated aquaporin-2 is targeted to the apical membrane of collecting duct principal cells. *Kidney Int.* **75,** 295–303
15. Moeller, H. B., Aroankins, T. S., Slengerik-Hansen, J., Pisitkun, T., and Fenton, R. A. (2014) Phosphorylation and ubiquitylation are opposing processes that regulate endocytosis of the water channel aquaporin-2. *J. Cell Sci.* **127,** 3174–3183
16. Kamsteeg, E. J., Hendriks, G., Boone, M., Konings, I. B., Oorschot, V., van der Sluijs, P., Klumperman, J., and Deen, P. M. (2006) Short-chain ubiquitination mediates the regulated endocytosis of the aquaporin-2 water channel. *Proc. Natl. Acad. Sci. U.S.A.* **103,** 18344–18349
17. Moeller, H. B., Praetorius, J., Rützler, M. R., and Fenton, R. A. (2010) Phosphorylation of aquaporin-2 regulates its endocytosis and protein-protein interactions. *Proc. Natl. Acad. Sci. U.S.A.* **107,** 424–429
18. Khositseth, S., Pisitkun, T., Slentz, D. H., Wang, G., Hoffert, J. D., Knepper, M. A., and Yu, M. J. (2011) Quantitative protein and mRNA profiling shows selective post-transcriptional control of protein expression by vasopressin in kidney cells. *Mol. Cell Proteomics* **10,** mcp.M110.004036
19. Loo, C. S., Chen, C. W., Wang, P. J., Chen, P. Y., Lin, S. Y., Khoo, K. H., Fenton, R. A., Knepper, M. A., and Yu, M. J. (2013) Quantitative apical membrane proteomics reveals vasopressin-induced actin dynamics in collecting duct cells. *Proc. Natl. Acad. Sci. U.S.A.* **110,** 17119–17124
20. Yu, M. J., Miller, R. L., Uawithya, P., Rinschen, M. M., Khositseth, S., Braucht, D. W., Chou, C. L., Pisitkun, T., Nelson, R. D., and Knepper, M. A. (2009) Systems-level analysis of cell-specific AQP2 gene expression in renal collecting duct. *Proc. Natl. Acad. Sci. U.S.A.* **106,** 2441–2446
21. Moeller, H. B., Olesen, E. T., and Fenton, R. A. (2011) Regulation of the water channel aquaporin-2 by posttranslational modification. *Am. J. Physiol. Renal Physiol.* **300,** F1062–1073
22. Huling, J. C., Pisitkun, T., Song, J. H., Yu, M. J., Hoffert, J. D., and Knepper, M. A. (2012) Gene expression databases for kidney epithelial cells. *Am. J. Physiol. Renal Physiol.* **302,** F401–407
23. Uawithya, P., Pisitkun, T., Ruttenberg, B. E., and Knepper, M. A. (2008) Transcriptional profiling of native inner medullary collecting duct cells from rat kidney. *Physiol. Genomics* **32,** 229–253

24. Yu, M. J., Pisitkun, T., Wang, G., Shen, R. F., and Knepper, M. A. (2006) LC-MS/MS analysis of apical and basolateral plasma membranes of rat renal collecting duct cells. *Mol. Cell Proteomics* **5,** 2131–2145
25. Tonikian, R., Zhang, Y., Sazinsky, S. L., Currell, B., Yeh, J. H., Reva, B., Held, H. A., Appleton, B. A., Evangelista, M., Wu, Y., Xin, X., Chan, A. C., Seshagiri, S., Lasky, L. A., Sander, C., Boone, C., Bader, G. D., and Sidhu, S. S. (2008) A specificity map for the PDZ domain family. *PLoS Biol.* **6,** e239
26. Noda, Y., Horikawa, S., Furukawa, T., Hirai, K., Katayama, Y., Asai, T., Kuwahara, M., Katagiri, K., Kinashi, T., Hattori, M., Minato, N., and Sasaki, S. (2004) Aquaporin-2 trafficking is regulated by PDZ-domain containing protein SPA-1. *FEBS Lett.* **568,** 139–145
27. Karthikeyan, S., Leung, T., and Ladias, J. A. (2002) Structural determinants of the Na^+/H^+ exchanger regulatory factor interaction with the β2-adrenergic and platelet-derived growth factor receptors. *J. Biol. Chem.* **277,** 18973–18978
28. Doyle, D. A., Lee, A., Lewis, J., Kim, E., Sheng, M., and MacKinnon, R. (1996) Crystal structures of a complexed and peptide-free membrane protein-binding domain: molecular basis of peptide recognition by PDZ. *Cell* **85,** 1067–1076
29. Harris, B. Z., and Lim, W. A. (2001) Mechanism and role of PDZ domains in signaling complex assembly. *J. Cell Sci.* **114,** 3219–3231
30. Mellman, I., and Nelson, W. J. (2008) Coordinated protein sorting, targeting and distribution in polarized cells. *Nat. Rev. Mol. Cell Biol.* **9,** 833–845
31. Lehmann, G. L., Benedicto, I., Philp, N. J., and Rodriguez-Boulan, E. (2014) Plasma membrane protein polarity and trafficking in RPE cells: past, present and future. *Exp. Eye Res.* **126,** 5–15
32. Cohen, N. A., Brenman, J. E., Snyder, S. H., and Bredt, D. S. (1996) Binding of the inward rectifier K^+ channel Kir 2.3 to PSD-95 is regulated by protein kinase A phosphorylation. *Neuron* **17,** 759–767
33. Cao, T. T., Deacon, H. W., Reczek, D., Bretscher, A., and von Zastrow, M. (1999) A kinase-regulated PDZ-domain interaction controls endocytic sorting of the β2-adrenergic receptor. *Nature* **401,** 286–290
34. Chetkovich, D. M., Chen, L., Stocker, T. J., Nicoll, R. A., and Bredt, D. S. (2002) Phosphorylation of the postsynaptic density-95 (PSD-95)/discs large/zona occludens-1 binding site of stargazin regulates binding to PSD-95 and synaptic targeting of AMPA receptors. *J. Neurosci.* **22,** 5791–5796
35. Hoffert, J. D., Pisitkun, T., Wang, G., Shen, R. F., and Knepper, M. A. (2006) Quantitative phosphoproteomics of vasopressin-sensitive renal cells: regulation of aquaporin-2 phosphorylation at two sites. *Proc. Natl. Acad. Sci. U.S.A.* **103,** 7159–7164
36. Richter, M., Murai, K. K., Bourgin, C., Pak, D. T., and Pasquale, E. B. (2007) The EphA4 receptor regulates neuronal morphology through SPAR-mediated inactivation of Rap GTPases. *J. Neurosci.* **27,** 14205–14215
37. Pak, D. T., Yang, S., Rudolph-Correia, S., Kim, E., and Sheng, M. (2001) Regulation of dendritic spine morphology by SPAR, a PSD-95-associated RapGAP. *Neuron* **31,** 289–303
38. Ding, G. H., Franki, N., Condeelis, J., and Hays, R. M. (1991) Vasopressin depolymerizes F-actin in toad bladder epithelial cells. *Am. J. Physiol.* **260,** C9–16
39. Riethmüller, C., Oberleithner, H., Wilhelmi, M., Franz, J., Schlatter, E., Klokkers, J., and Edemir, B. (2008) Translocation of aquaporin-containing vesicles to the plasma membrane is facilitated by actomyosin relaxation. *Biophys. J.* **94,** 671–678
40. Klussmann, E., Tamma, G., Lorenz, D., Wiesner, B., Maric, K., Hofmann, F., Aktories, K., Valenti, G., and Rosenthal, W. (2001) An inhibitory role of Rho in the vasopressin-mediated translocation of aquaporin-2 into cell membranes of renal principal cells. *J. Biol. Chem.* **276,** 20451–20457
41. Tamma, G., Klussmann, E., Procino, G., Svelto, M., Rosenthal, W., and Valenti, G. (2003) cAMP-induced AQP2 translocation is associated with RhoA inhibition through RhoA phosphorylation and interaction with RhoGDI. *J. Cell Sci.* **116,** 1519–1525
42. Yui, N., Lu, H. J., Bouley, R., and Brown, D. (2012) AQP2 is necessary for vasopressin- and forskolin-mediated filamentous actin depolymerization in renal epithelial cells. *Biol. Open* **1,** 101–108
43. Heissler, S. M., and Manstein, D. J. (2013) Nonmuscle myosin-2: mix and match. *Cell. Mol. Life Sci.* **70,** 1–21
44. Araki, N. (2006) Role of microtubules and myosins in Fcγ receptor-mediated phagocytosis. *Front. Biosci.* **11,** 1479–1490
45. Olazabal, I. M., Caron, E., May, R. C., Schilling, K., Knecht, D. A., and Machesky, L. M. (2002) Rho-kinase and myosin-II control phagocytic cup formation during CR, but not FcγR, phagocytosis. *Curr. biol.* **12,** 1413–1418
46. Chou, C. L., Christensen, B. M., Frische, S., Vorum, H., Desai, R. A., Hoffert, J. D., de Lanerolle, P., Nielsen, S., and Knepper, M. A. (2004) Non-muscle myosin II and myosin light chain kinase are downstream targets for vasopressin signaling in the renal collecting duct. *J. Biol. Chem.* **279,** 49026–49035
47. Chou, C. L., Yu, M. J., Kassai, E. M., Morris, R. G., Hoffert, J. D., Wall, S. M., and Knepper, M. A. (2008) Roles of basolateral solute uptake via NKCC1 and of myosin II in vasopressin-induced cell swelling in inner medullary collecting duct. *Am. J. Physiol. Renal Physiol.* **295,** F192–201
48. Yang, C. R., Tongyoo, P., Emamian, M., Sandoval, P. C., Raghuram, V., and Knepper, M. A. (2015) Deep proteomic profiling of vasopressin-sensitive collecting duct cells: I. virtual Western blots and molecular weight distributions. *Am. J. Physiol. Cell Physiol.* **309,** C785–798
49. Yang, C. R., Raghuram, V., Emamian, M., Sandoval, P. C., and Knepper, M. A. (2015) Deep proteomic profiling of vasopressin-sensitive collecting duct cells: II. bioinformatic analysis of vasopressin signaling. *Am. J. Physiol. Cell Physiol.* **309,** C799–812
50. Noda, Y., and Sasaki, S. (2006) Regulation of aquaporin-2 trafficking and its binding protein complex. *Biochim. Biophys. Acta* **1758,** 1117–1125
51. Noda, Y., and Sasaki, S. (2008) The role of actin remodeling in the trafficking of intracellular vesicles, transporters, and channels: focusing on aquaporin-2. *Pflugers Arch.* **456,** 737–745
52. Barile, M., Pisitkun, T., Yu, M. J., Chou, C. L., Verbalis, M. J., Shen, R. F., and Knepper, M. A. (2005) Large scale protein identification in intracellular aquaporin-2 vesicles from renal inner medullary collecting duct. *Mol. Cell Proteomics* **4,** 1095–1106
53. Schneider, C. A., Rasband, W. S., and Eliceiri, K. W. (2012) NIH Image to ImageJ: 25 years of image analysis. *Nat. Methods* **9,** 671–675
54. Sali, A., and Blundell, T. L. (1993) Comparative protein modelling by satisfaction of spatial restraints. *J. Mol. Biol.* **234,** 779–815
55. London, N., Raveh, B., Cohen, E., Fathi, G., and Schueler-Furman, O. (2011) Rosetta FlexPepDock web server: high resolution modeling of peptide-protein interactions. *Nucleic Acids Res.* **39,** W249–253
56. Jorgensen, W. L., Maxwell, D. S., and Tirado-Rives, J. (1996) Development and testing of the OPLS all-atom force field on conformational energetics and properties of organic liquids. *J. Am. Chem. Soc.* **118,** 11225–11236
57. Kaminski, G. A., Friesner, R. A., Tirado-Rives, J., and Jorgensen, W. L. (2001) Evaluation and parametrization of the OPLS-AA force field for proteins via comparison with accurate quantum chemical calculations on peptides. *J. Phys. Chem. B* **105,** 6474–6487
58. Laskowski, R. A., MacArthur, M. W., Moss, D. S., and Thornton, J. M. (1993) PROCHECK: a program to check the stereochemical quality of protein structures. *J. Appl. Cryst.* **26,** 283–291